Phase Behavior of the Supercooled Aqueous Solutions of Dimethyl Sulfoxide, Ethylene Glycol, and Methanol As Seen by Dielectric Spectroscopy

S. S. N. Murthy

School of Physical Sciences, Jawaharlal Nehru University, New Delhi 110 067, India

Received: February 5, 1997; In Final Form: May 23, 1997[⊗]

The dielectric behavior of the supercooled aqueous solutions of dimethyl sulfoxide (DMSO), ethylene glycol (EG), and methanol (MeOH) has been examined in the frequency range 10^6-10^{-3} Hz and in the x_m range of 0.19−0.40, 0.25−0.85, and 0.50−0.85, respectively, where x_m is the mole fraction of the second component. Differential scanning calorimetric measurements have also been carried out on the samples. At temperatures above the glass transition temperature (T_g), it was found that the Hevriliak−Negami relaxation function is appropriate to describe the data. The "apparent" distribution in relaxation times increases with increasing water content and also on lowering the temperature. But at temperatures just above T_g, an Arrhenius branch of considerable polarization and with an activation energy of ∼21.5 kJ/mol separates out to continue to the sub-T_g region, which more or less disappears around $x_m = 0.33$ in DMSO solutions and around $x_m = 0.50$ in EG solutions. It is suggested that the complexes of 2:1 (in DMSO solutions) and 1:1 (in EG solutions) are present in the liquid that are thermolabile and exist in an undissociated state only near T_g, and the sub-T_g process is due to the relaxation of water molecules. No evidence of complex formation is found in MeOH solutions.

Introduction

The study of aqueous solutions is currently receiving a lot of attention in view of the suspected micelle-like structures on the water-rich side which are considered as reference systems for more complicated aqueous systems like surfactants, emulsions, and biopolymers.[1−5] Dimethyl sulfoxide (DMSO) in aqueous solutions is one of the few systems that have been studied very widely using different techniques, in view of its unique biological properties[6] and the wide use of its solutions as solvents and reaction media[8] and its use as a cryoprotectant.[7] However, there is no agreement in the way it interacts with water, although it is well-known that the water−DMSO hydrogen bond is stronger than the H-bond between water molecules.[9] However, it is generally accepted that in the mole fraction range $x_m = 0.3-0.4$ of DMSO the DMSO−water interactions due to hydrogen bonds are at a maximum. What is not clear is whether this interaction results in formation of complexes.[10−15] For example, the viscosity (or dielectric relaxation time)[15−22] data shows a maximum at $x_m = 0.33$, which is taken as evidence[12,13] for a 2:1 complex of water and DMSO. But the infrared (IR) studies[23,24] and Raman studies[10] do not support this view. When the viscosity measurements are extended to lower temperatures, the peak intensity is found[12,14] to increase. Therefore, it is suggested[12] that the complexes are thermolabile in nature. If that is so, then the stability and the lifetime of such complexes have to be addressed.

Kaatze et al.[15] have tried to study these points by performing microwave dielectric measurements at room temperature. Although they could not find evidence for the existence of stoichiometrically well-defined water−DMSO aggregates, the dielectric spectra showed two maxima (one each on the water-rich side and DMSO-rich side) in the distribution of relaxation times against concentration and a minimum around $x_m = 0.33$, indicating more homogeneity around $x_m = 0.33$. The recent phase diagram (PD) studies carried out in this laboratory[25] indicated two complexes of 3:1 and 2:1 of water−DMSO. (An earlier PD study of Rasmussen and MacKenzie[26] indicated a 3:1 complex and some metastable complex around $x_m = 0.33$.) However, what is not clear from the PD study is the stability of the complexes as the material goes from the solid to liquid state, since the apparent melting temperatures are found to be not too different from the corresponding eutectic temperatures. Hence, it is felt that the study of these solutions in the supercooled state may be of some help because the stoichiometrically well-defined complexes are expected to give well-separable contributions to the dielectric spectrum in the high-viscosity regime, which may in turn give some indication about the stability (or lifetime) of the complexes.

The other binary system that behaves more or less like water−DMSO in the PD study is the water−ethylene glycol (EG) system, which shows a 1:1 complex formation.[25] The corresponding viscosity data[27] at room temperature, however, do not show any peak. It may be argued that the contribution of the complex to the viscosity is not sufficient enough to be revealed as a peak or that the stability of the complexes formed is so weak that they do not exist at room temperature. In order to answer the question of the stability of the complexes in these aqueous solutions, it is desirable to extend the dielectric measurements to low temperatures, which is proposed to be done in this article.

Experimental Section

The water used in this study is reagent grade deionized water and is obtained from M/s. Reckon Diagnostics Pvt. Ltd., India. Water obtained from M/s. E. Merck, Germany, is also used. The details of the other chemicals used in this study are as follows: dimethyl sulfoxide (DMSO) (HPLC, M/s. Spectrochem, India); ethylene glycol (EG) (LR, M/s. S.d. Fine Chem Ltd., India), and methyl alcohol (MeOH) (HPLC, M/s. CDH, India).

In this study an HP4284A precision LCR Meter (frequency range $20-10^6$ Hz) is used for the dielectric measurements, and a time domain step-response technique is used for the frequency range $10^{-0.6}-10^{-3.0}$. DSC involving a DuPont 2000 TA system

[⊗] Abstract published in *Advance ACS Abstracts,* July 1, 1997.

S1089-5647(97)00451-3 CCC: $14.00

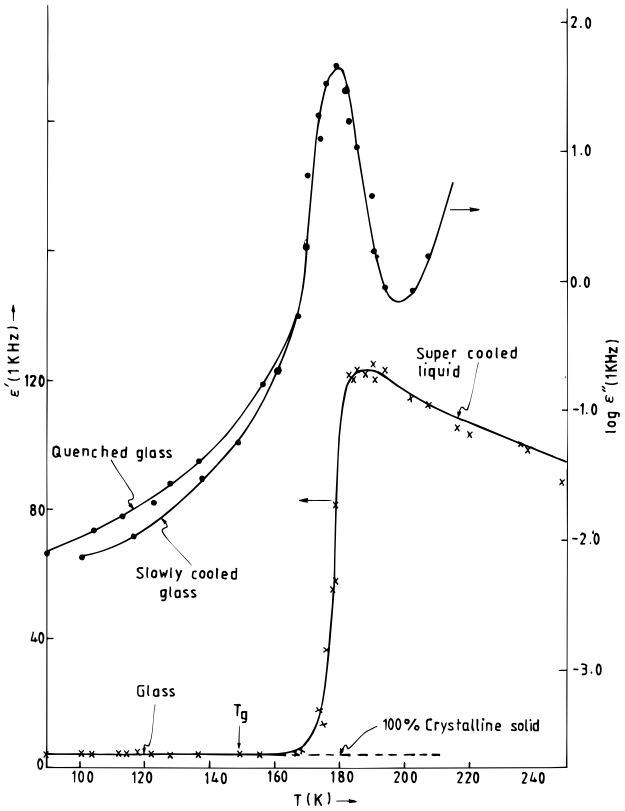

Figure 1. Variation of the real and imaginary parts (ϵ', ϵ'') of the complex dielectric constant at 1 kHz test frequency with temperature for both the supercooled and the glassy states of DMSO aqueous solution with $x_m = 0.25$. Also shown is the ϵ' variation of the corresponding completely crystallized state for comparison sake. Two sets of data are included: one for the slowly cooled sample and the other for the rapidly cooled sample.

with a quench cooling accessory is used as a supporting technique. For further details of these techniques, their accuracy, and temperature control, the reader may consult the earlier publications[28,29] from this laboratory.

The electrodes used for the dielectric study are nickel-plated brass electrodes. In the case of DMSO solutions at temperatures above 190 K large ionic conductance and electrode polarization comes into the picture, making the determination of the static dielectric constant (ϵ_0) difficult. It is noticed that the electrode polarization appearing above 190 K can be eliminated by using platinum or gold electrodes, but because of the difficulty in maintaining the interelectrode distance in this thin electrode assembly, the measurement of ϵ_0 was abandoned above 190 K.

Results

For the sake of convenience, the Results section is structured into subsections in the following way.

(a) The Aqueous Solutions of DMSO. These solutions can be supercooled easily only in solutions with mole fractions of DMSO (x_m) from 0.19 to 0.40,[26] and hence, the dielectric measurements are performed in the supercooled and glassy states only in solutions. At temperatures of about 15−20 K above T_g, the main relaxation process appears in the bridge frequency region, and only one relaxation process is found in the frequency region above 77 K. This situation is shown in Figure 1, where the variation of both the real and imaginary parts of the dielectric constant, ϵ' and ϵ'', at 1 kHz test frequency are shown as a function of temperature for the sample with $x_m = 0.25$. Below T_g, the value of ϵ' is found to be almost frequency independent, and this value is approximately 3.6, which is close to that of

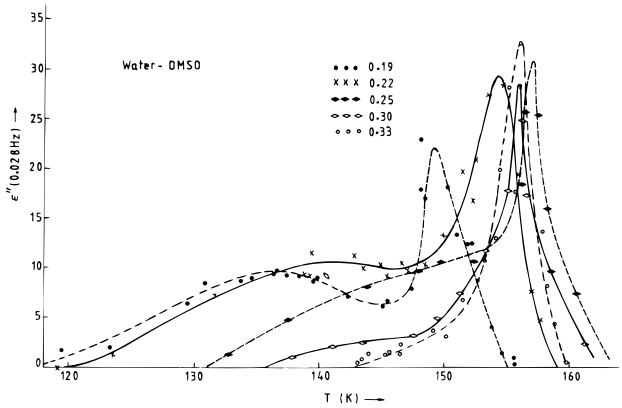

Figure 2. Variation of dielectric loss (ϵ'') at a fixed frequency of 0.028 Hz with temperature for different x_m values of the aqueous solutions of DMSO.

the completely crystallized sample but is much greater than the corresponding square of the refractive index (n_D^2). (The n_D value at room temperature is 1.423[12] for this sample, and in view of its known weak temperature dependence, one can approximate the n_D value at lower temperatures to be more or less the same. Thus, the n_D^2 value is expected to be about 2.02.) When the temperature of the sample approaches the T_g, the dispersion moves to ultralow frequencies and splits into two processes, as shown in Figure 2.

The complex permittivity data in the LCR bridge frequency range can be described by the Havriliak−Negami equation[30] given by

$$\frac{\epsilon^*(f) - \epsilon_\infty}{(\epsilon_0 - \epsilon_\infty)} = [1 + (i(f/f_0))^{1-\alpha}]^{-\beta} \quad (1)$$

where α and β are the geometric shape parameters (sometimes described as the symmetric and asymetric distribution parameters, respectively) and f_0 is the mean relaxation frequency.

In the above equation ϵ_∞ is the high-frequency limit of the dispersion, which in the present case of aqueous DMSO solutions is about 5.0. Such a large deviation of ϵ_ω from the n_D^2 value is found even in water[31,32] and may other strongly polar liquids.[33] In Figure 3a, the audio frequency dispersions for all the aqueous DMSO solutions are shown in the form of normalized complex plane diagrams. The data shown in Figure 3a, at each temperature, can be represented by eq 1 within experimental accuracy. However, the data at the lowest temperature side for samples with $x_m = 0.19$, 0.22, and 0.25 slightly deviate from eq 1, and the corresponding fits are not as good as the ones at higher temperatures. The lower temperature process (or sub-T_g process) is found to obey the Cole−Cole dispersion equation,[33] which is a limiting form of eq 1 for $\beta = 1$, for which f_0 tends to be the peak loss frequency f_P. The corresponding value of α is found to be approximately 0.3, and corresponding $\Delta\epsilon$ ($\epsilon_0 - \epsilon_\infty$) values are given in Table 1 (the suffix "cc" is added to α in Table 1 in order to identify it as the limiting case of $\beta = 1$ in eq 1). These $\Delta\epsilon$ values when compared with the corresponding values of dispersion shown in Figures 1, 2, and 3a reveal that about 25% of the total polarization above T_g is associated with the secondary process for lower x_m values in DMSO solutions with $x_m \leq 0.25$. In addition, the f_P values corresponding to the sub-T_g process are found to follow the Arrhenius equation.

$$f_P = f_A \exp(-E/RT) \quad (2)$$

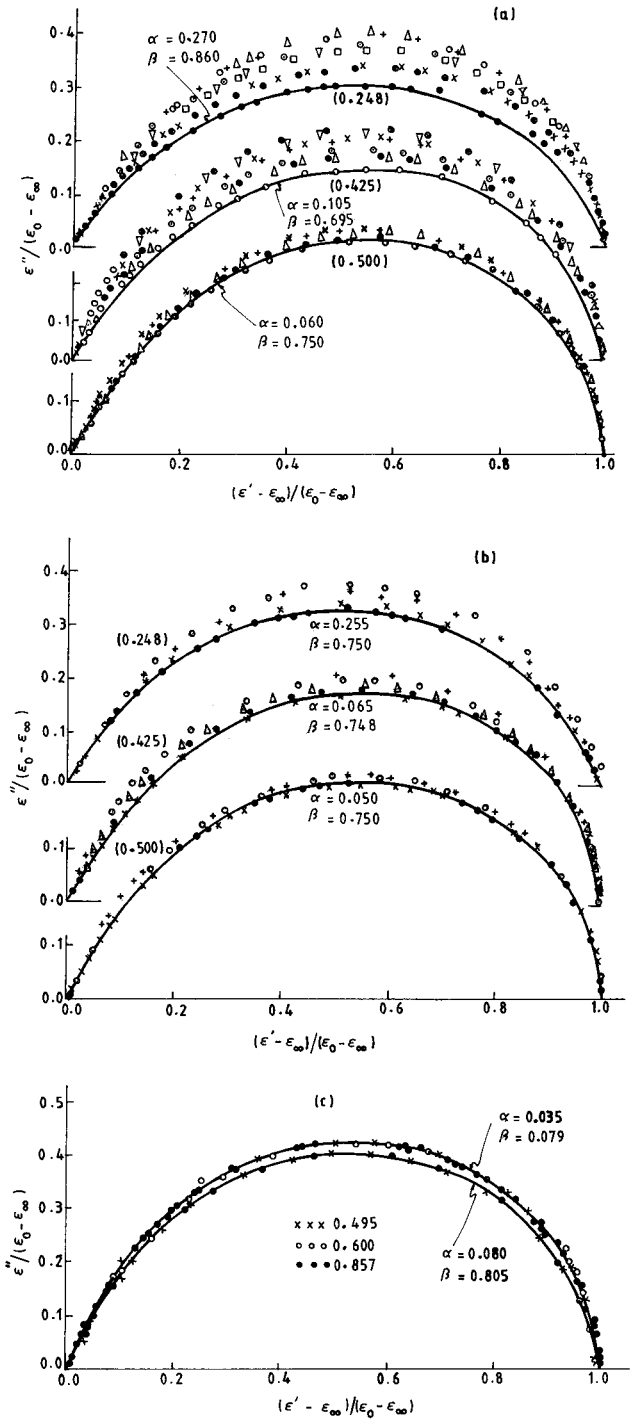

Figure 3. Normalized C−C plots in aqueous solutions of (a) DMSO, (b) EG, and (c) MeOH for various x_m values and at various temperatures. The thick lines correspond to the H−N fit (eq 1) to the data at the lowest temperature in the range shown below, and the corresponding parameters are shown along the fits. The temperature range corresponds to (a) $x_m = 0.19$ (165.7−184.0 K); 0.25 (166.5−184.7 K); 0.33 (173.2−183.1 K); (b) $x_m = 0.248$ (170.9−185.2 K); 0.425 (175.4−198.7 K); 0.50 (175.7−193.2 K); (c) $x_m = 0.495$ (150−160 K); 0.6 (143−153 K); 0.857 (125.2−132.2 K).

where E is the corresponding activation energy per mole and f_A is the preexponential factor. These details are also included in Table 1.

The shape of the primary process near T_g is not clear because of the presence of the secondary (sub-T_g) process. The peak loss frequency f_P corresponding to the primary process in the audio frequency range is obtained with the help of f_0 of eq 1 through the approximate[33b] identity $f_P = f_0 \tan[\pi/2(1 + \beta)]$. All the f_P values of the primary and the sub-T_g process are plotted against temperature in the form of an Arrhenius diagram, as shown in Figure 4a, where the microwave data of others are also included. The DSC curves near T_g are critically examined (Figure 5a) for the sub-T_g process. Indeed, the curves with $x_m < 0.3$ reveal a diffused steplike change on the lower temperature end of the DSC scans.

TABLE 1: Details of the Sub-T_g Process

x_m	E (KJ/mol)	log f_A (Hz)	range of temperature (K)	range of α_{cc}	range of $\Delta\epsilon$ ($\epsilon_0 - \epsilon_\infty$)
			Water−DMSO		
0.190	19.67	5.69	129−145	0.30−0.32	30−36
0.220	23.48	6.90	132−145	0.30−0.35	32−42
0.250	21.07	5.56	138−149	0.29−0.4	31−34
			Water−EG		
0.248	24.40	6.97	134.49		
0.425	22.57	5.80	140−152		

(b) The Aqueous Solutions of EG. These solutions can be supercooled very easily for the mole fraction (x_m) of EG in the range 0.25−0.85,[25,36] where the dielectric measurements can be performed. As in the case of the DMSO solutions, as shown in Figure 1, the bridge frequency range shows only one relaxation process, which splits into two processes at much lower frequencies at temperatures near T_g (Figure 6). The process found in the audio frequency range can be described by eq 1, and this situation is shown in Figure 3b, where the data over the x_m values of 0.25−0.85 are shown in the form of normalized C−C diagrams. The shape of the C−C diagrams shows a large variation with temperature for lower x_m values, as in the case of DMSO solutions. Figure 4b depicts the complete Arrhenius diagram. The actual shape of the sub-T_g process cannot be ascertained definitely because of its proximity to the main relaxation process at T_g, and hence, the corresponding peak loss frequency values shown in Figure 4b are approximate. The freezing of the sub-T_g process can be seen in the DSC curves below T_g as a small steplike change, which gradually disappears as one moves to higher x_m values (Figure 5b).

(c) Aqueous Solutions of MeOH. The dielectric measurements can only be performed in the supercooled state for the mole fraction range (x_m of MeOH) 0.5−0.85 without the intervention of crystallization. The data corresponding to this mole fraction range are shown in Figure 3c in the form of normalized C−C diagrams, and the complete Arrhenius plot is shown in Figure 4c. Unlike the aqueous solutions of DMSO and EG, the sub-T_g region could not be critically examined because of the (lower) temperature limitation in the DSC experiment.

The variation of the shape parameters α and β of eq 1 with x_m is shown in Figure 7 for all the samples. The variation of the dielectric relaxation time τ defined as $(2\pi f_P)^{-1}$ at a given temperature with x_m is shown in Figure 8 and the variation of calorimetric T_g with x_m is shown in Figure 9 for all the samples. It is noticed that the f_P values corresponding to the main relaxation process in the supercooled solutions more or less follow the power-law equation of the form[28]

$$f_P = f_B \left(\frac{T - T'_g}{T'_g} \right)^r \qquad (3)$$

where T'_g is the zero relaxation frequency temperature; r is the dynamic exponent. For DMSO solutions, the f_P values are a little scattered, and hence, the values of the parameters of eq 3 given in Table 2 are the average values of at least three runs.

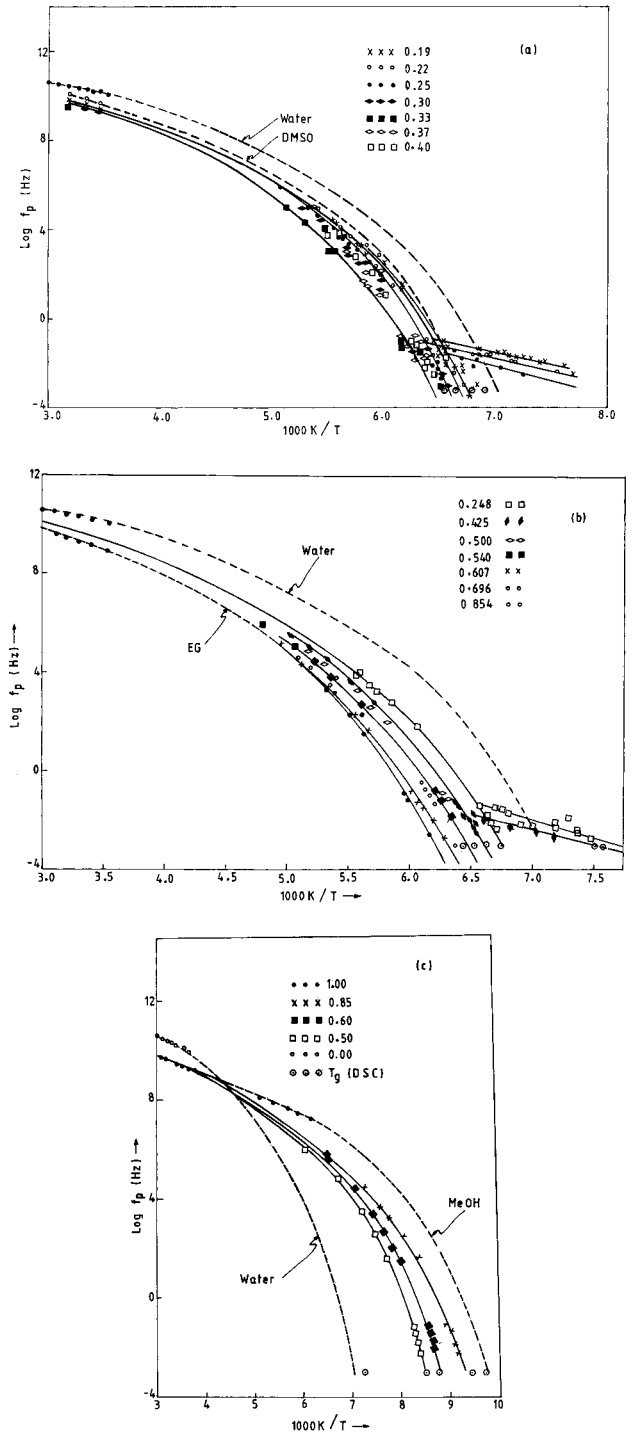

Figure 4. Arrhenius plot for the peak loss frequency f_P in aqueous (a) DMSO, (b) EG, and (c) MeOH solutions. The curve corresponding to DMSO in a and MeOH in c is hypothetical and is constructed with the help of the microwave data[15,22,35] and the (extrapolated) T_g value.[34,36] The curve for water is constructed in a similar fashion with the help of the microwave data[35] and the f_P, values obtained by Huch et al.[32] for the supercooled water by extrapolation of the aqueous solutions of glycerol. The points shown by the symbol ⊙ correspond to the enthalpy relaxation data (i.e., DSC). Also included is the microwave data of others.[15,22,37]

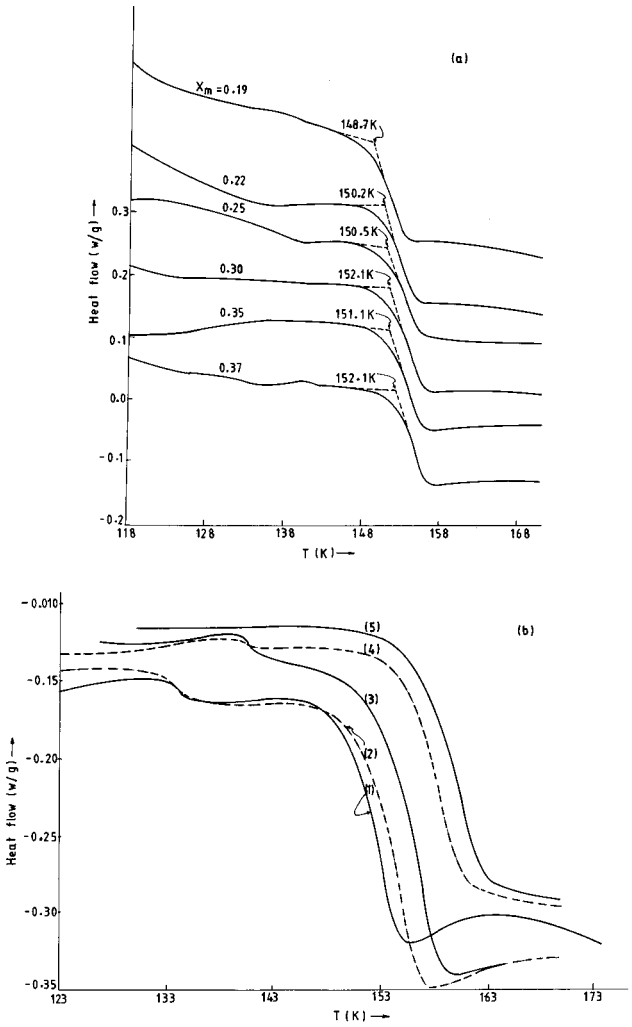

Figure 5. DSC curves for a heating rate of 10 K/min in the region of T_g in the aqueous solutions of (a) DMSO and (b) EG. (The samples are cooled normally at a rate of about 5 K/min to 100 K before taking the DSC curve.) Note that there is a tendency to have a diffused steplike, change in part a and a small but clear steplike change in part b below T_g which disappears for $x_m > 0.33$ in part a and for $x_m > 0.5$ in part *b*. The sample size with increasing x_m values is (a) 12.6 mg, 12.3 mg, 23.4 mg, 17.1 mg, 13.1 mg, and 13.1 mg, respectively, and (b) 12.9 mg, 13.5 mg, 16.8 mg, 26.1 mg, and 15 mg.

Discussion

For the sake of covenience, the discussion part is divided into a few sections.

1. Sub-T_g Process. When a single-component liquid is cooled fast enough to form glass, some molecular mobility (β-process) is still found in the glassy state which is intramolecular in origin.[39] (In a polymeric glass, this mobility is the segmental motion involving not more than four to five carbon atoms, and in an organic glass with a flexible dipolar side group, it is the hindered side group rotation.) The domination of this process in the sub-T_g dielectric measurements depends on the polarity of the rotating entity. Thus, one can expect a less intense β-process, for example, in 3-bromopentane (where the dipole is mainly on the third carbon atom) as compared to a glass formed of 1-bromopentane because in the latter the end group is expected to contribute significantly to the dielectric measurements. Similarly in the case of glasses formed of carbohydrates,[40] such as glucose, a strong β-process is found from the segmental motions because of the presence of a large number of strong polar −OH groups on the segments. However, the situation is different in a glass formed by supercooling a binary liquid.[29] Here an additional sub-T_g process can be expected due to the hindered movement of the smaller component molecules in the local cages or interstices created by the glassy matrix. This is an intermolecular process and, hence, reflects the size and shape of the rotating component molecules.[41] Its magnitude is expected to be larger for smaller molecules. In this case the activation energy of the sub-T_g process is expected

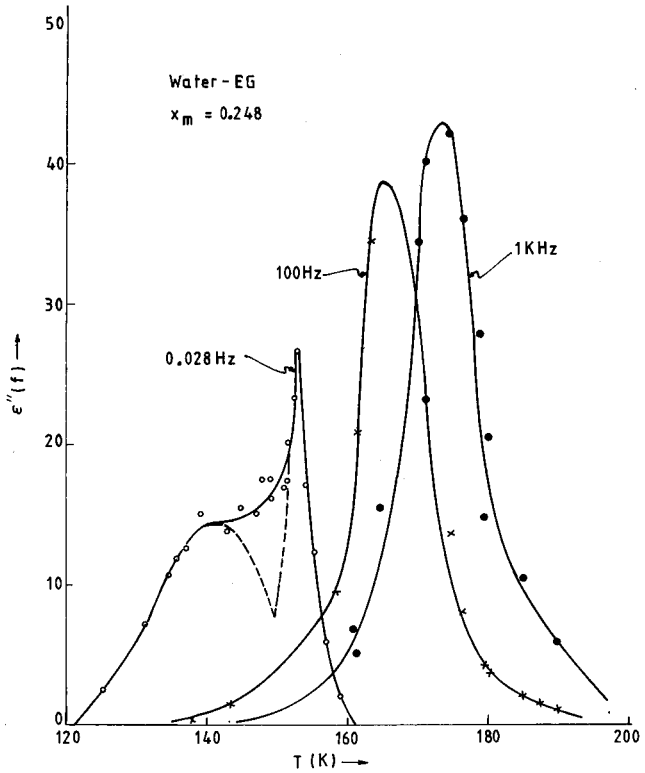

Figure 6. Variation of dielectric loss (ϵ'') at fixed frequencies with temperature in the aqueous solution of EG with $x_m = 0.248$. Note that the curve for $f = 0.028$ Hz can be expressed as a superposition of two processes as shown by the dashed line.

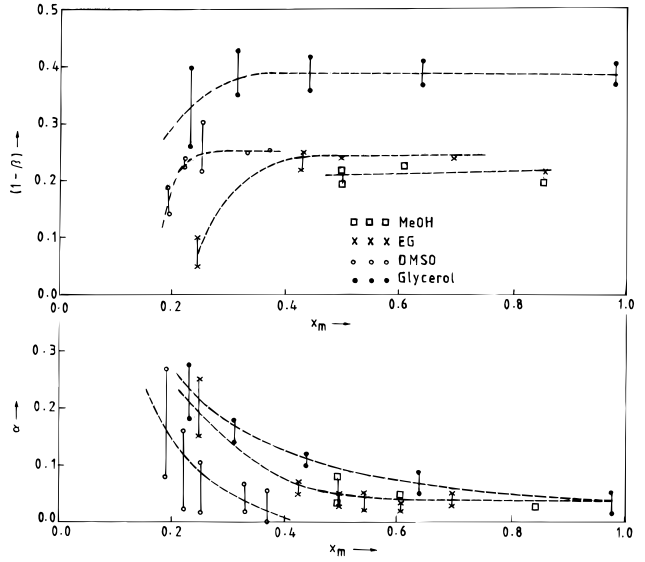

Figure 7. Variation of the H−N shape parameters α and $(1 - \beta)$ with x_m. The vertical lines through the points correspond to the temperature variation of these parameters in the temperature range where the bridge frequency data show a well-defined peak in ϵ'' as revealed in Figure 3 and 4. Also shown are the data corresponding to the aqueous solutions of glycerol taken from Table 1 of ref 32.

to be not too different from the corresponding value found for the true liquid state of the solute. In this context, it is very interesting to note that the activation energy found for the sub-T_g process in the aqueous solutions shown in Table 1 is not too different from the activation energy of ∼21 kJ/mol found for liquid water.[31] Moreover, the sub-T_g process decreases in its magnitude with decrease of water concentration (or increase of x_m values; see Figures 2 and 6).

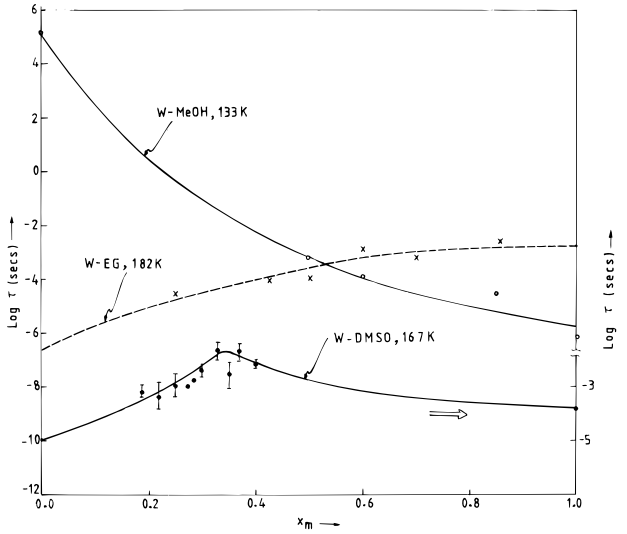

Figure 8. Variation of relaxation time τ $(=2\pi f_P)^{-1}$ at a constant temperature with x_m values in the supercooled region.

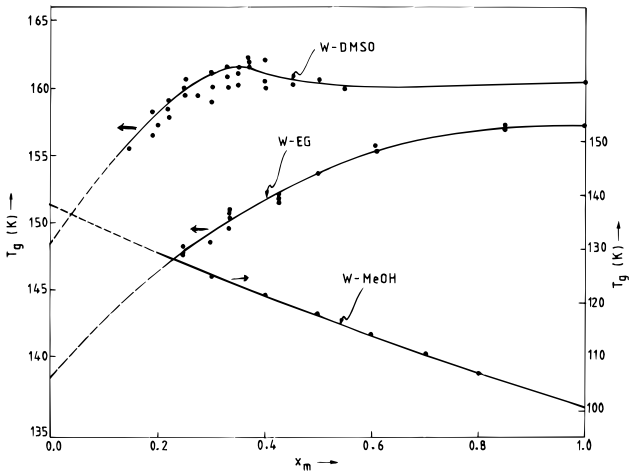

Figure 9. Variation of the calorimetric T_g (or simply T_g) with x_m in the systems studied. The curve corresponding to the DMSO solutions is shifted vertically by 10 K to avoid overlap with the other curves. The data for these solutions correspond to different runs. Part of the data corresponding to aqueous MeOH solutions is taken from ref 34.

TABLE 2: Details of the Main Relaxation Process

x_m	T'_g	r	log f_B
	Water−DMSO		
0.19	133.5	15.11	11.45
0.25	134.5	18.47	13.33
0.30	135.0	15.96	11.51
0.33	137.0	16.17	11.49
0.37	136.0	19.74	13.82
	Water−EG		
0.248	132.0	14.13	10.00
0.425	136.0	14.50	10.49
0.500	136.0	14.18	10.19
0.607	138.0	17.12	10.93
0.696	140.0	12.61	9.39
	Water−MeOH		
0.500	112	9.43	9.20
0.855	100	10.02	8.36

The two points just mentioned above are strong evidences to suggest that the sub-T_g process in the aqueous solutions of DMSO and EG are due to the relaxation of water molecules. (The Maxwell−Wagner polarization is ruled out, as the sub-T_g process is found even in the enthalpy relaxation data shown in Figure 5.) The other possible mechanism is a liquid immiscibil-

ity just above T_g with one of the liquids surviving below the T_g of the first liquid. However, if one looks at Figure 4a,b, one would realize that the sub-T_g process is strictly Arrhenius, and the small steplike change found at temperatures below the T_g of the solutions in Figure 5 corresponds to the freezing of the Arrhenius branch of Figure 4a,b. This rules out the liquid immiscibility as a possible mechanism because a phase-separated liquid reveals itself in two non-Arrhenius relaxation processes characteristic of the each separated liquid component.

The liquid viscosity at which the bifurcation of the liquid relaxation is occurring whereby one relaxation process evolves as an Arrhenius process (as in Figure 4a,b) is expected to be on the order of $10^{10}-10^{11}$ P, comparable to that of a (near) solid, and hence one may also be tempted to explain the sub-T_g process as due to the one seen[42] in hexagonal ice. Moreover, the sub-T_g process is seen as a major event in the dielectric measurements amounting to about 20−25% of the total polarization around T_g (see Table 1). But the same process is not seen as a major event in the enthalpy relaxation data shown in Figure 5. However, the activation energy found for the relaxation process in hexagonal ice (I_h) is ∼55.5 kJ/mol,[42] which is much greater than the corresponding value for the sub-T_g process. This discourages the interpretation of the mechanism for the sub-T_g process along the lines of that found in hexagonal ice. Thus, it appears that the sub-T_g process is due to the rotation of water molecules in the interstices of the glass. However, the preexponential factor f_A in eq 2 (see Table 1) is lower by a few decades than the usual lattice vibrational frequency to $10^{12}-10^{3}$ Hz, which needs an explanation.

2. The Shape of the C−C Diagrams. Many of the simple component liquids show a Cole−Davidson (C−D) type ($\alpha = 0$ in eq 1) of relaxation in the supercooled regime.[33,39,43,44] Deviations from $\alpha = 0$ in eq 1 are found in some organic liquids which have some contribution to the polarization from the intramolecular rotation.[43,44] Similarly in polymers, a nonzero α results from different segmental motions.[45] A nonzero α is also found in binary liquids in the supercooled region.[29,46] Clear deviation from C−D type behavior is also seen in some aqueous solutions even at room temperature.[37,47]

As shown in Figure 3a,b, in the solutions of DMSO and EG, large deviations from $\alpha = 0$ are noticed, which increase with increasing water content. More interesting is the rapid increase of α in the supercooled region as the temperature is lowered, especially on the water-rich side. The present results and the room temperature results of Kaatze et al.[15] clearly show this trend. For example, in the DMSO solutions with $x_m = 0.33$; the $(1 - \beta)$ value is 0.113 at room temperature, and this increase to 0.25 in the supercooled state, whereas the corresponding α varies from zero to 0.06 only (see Figures 3a and 7). For $x_m = 0.20$, $(1 - \beta)$ varies from 0.13 at room temperature to 0.21 in the supercooled state and the corresponding variation of α is from zero to 0.25. Interestingly the overall temperature variation of the shape of the C−C diagram is minimal for $x_m = 0.33$ in DMSO solutions, and beyond $x_m = 0.33$, it has a tendency to increase further. This variation with concentration is in line with the room-temperature measurement of Kaatze et al.,[15] where the deviations from the Debye behavior are maximum around $x_m \approx 0.09$ and 0.85 with a minimum at $x_m \approx 0.33$. Although the room-temperature data are not available, the EG solutions also show a similar trend in the supercooled state around $x_m \approx 0.50$. Thus, the solutions appear to be more homogeneous around $x_m = 0.33$ in DMSO solutions and around $x_m = 0.5$ in EG solutions. It is interesting to note that at these concentrations the equilibrium PD shows compound formation (for more details see ref 25) and the magnitude of the sub-T_g processes is almost zero (see Figures 2 and 6). Thus, it appears that at these concentrations most of the molecules are associated in 2:1 and 1:1 complexes in the DMSO and EG solutions, respectively, at temperatures close to T_g. However, the existence of the metastable states in the PD[25] shows the presence of free water around these concentrations at temperatures above 210 and 198 K, respectively, in the EG and DMSO solutions. This implies that the complexes present in the solutions are somewhat thermolabile and exist in a dissociated state in the liquid at higher temperatures. However, the dielectric behavior of these liquids in the supercooled state at temperatures much below 210 K for $x_m = 0.33$ (in DMSO solutions) and $x_m = 0.50$ (in EG solutions) is more like that of a single-component (monomeric) liquid, indicating a more stable complex at temperatures near T_g. For concentrations less than 0.33 in DMSO solutions or 0.50 in EG solutions, the supercooled liquids can be thought of as mixtures of water and the complex, with water revealing itself as a sub-T_g process at these concentrations. Here the sub-T_g process is more like that found in binary liquids with the water molecules retaining their orientational freedom to some extent in the frozen glassy matrix formed.

Apart from the evidence given by the metastable states in the PD for the thermolabile nature of the complexes present in the solution, the other evidence comes from the τ vs x_m curves, which show a peak around $x_m = 0.33$ in DMSO solutions, with the peak intensity increasing sharply toward the lower temperature side. (This can be seen by comparing the peak intensity of the curve corresponding to the DMSO solutions in Figure 8 with that of the room-temperature data of Kaatze et al.[15]) In the case of an "ideal" mixture one would expect the relaxation time τ of the mixtures to be

$$\log \tau = x_m \log \tau_2 + (1 - x_m) \log \tau_1 \qquad (4)$$

where τ_1 and τ_2 are the relaxation times of the pure components. The above equation is based on the assumption that relaxation time follows the rate equation, and the free energy of activation of the components follows the mixture rule.[37] Similarly one should expect the T_g of the "ideal" solution to follow a similar equation[48] of the type given by eq 4 by writting T_g's for log τ's as

$$T_g = x_m T_{g1} + (1 - x_m) T_{g2} \qquad (5)$$

where T_{g1} and T_{g2} are the glass transition temperatures of the components of the mixture.

Equation 4 results in a straight line if log τ is plotted against x_m. Positive deviations from the above equation often result from complex formation.[13] However, interaction between the component molecules can also result in a positive deviation.[15,38] Large positive deviation can result in a peak in the plot of τ vs x_m. In a recent publication[25] from this laboratory, it was shown that in the case of aqueous solutions such peaks result from the presence of complexes or from ice clathrate-like structures in the liquid state. In the present case of DMSO solutions, the peak in the log τ vs x_m curve found in the data[15] at room temperature increases many-fold at lower temperatures (Figure 8), indicating the thermolabile nature of the complex formed. The plot of T_g vs x_m also has a tendency to show a peak around $x_m = 0.33$ in DMSO solutions (Figure 9), and there is an unusual scatter in the measured T_g values probably because of the thermolabile nature of the complex, the lifetime of which is probably comparable to the DSC time scale. In EG solutions, although, there is a tendency for a peak in the log τ vs x_m (Figure 8), no clear peaks are found for these solutions in either Figure 8 or Figure 9, most probably because the contribution from the

complex does not lead to a peak. In MeOH solutions, negative deviations from eq 4 or eq 5 are noticed in Figures 8 and 9, indicating that no complexes are formed in the supercooled liquids, which is also supported by study of the PD of this system.[25] It is interesting to see that the recent thermodynamic investigations[49−51] of these solutions reveal a change in the mixing scheme at the compositions corresponding to the complexes. In the case of methanol[51] the transition point in the mixing scheme, which is at $x_m = 0.16$ (which corresponds to the clathrate composition in our PD study[25]), could not be verified in our dielectric study, as these solutions with $x_m < 0.45$ could not be supercooled below without the intervention of crystallization.

Conclusions

The dielectric study of the aqueous solution of DMSO and EG in their supercooled state along with the PD study indicates that they behave more like three-component liquids at higher temperature where the concentrations of the component change with temperature because of the unstable nature of the complexes formed. Where the temperature is lowered toward T_g, the stability of the complexes increases and the solutions start behaving more like a mixture of two component liquids: the components being the stable complex and the "excess" water or the nonaqueous component. The glass then formed of these solutions follows the mixture rule of one each for the water-rich side and the nonaqueous component-rich side. On the water-rich side, the "excess" or "free" water molecules retain their orientational degree of freedom to some extent even below T_g because of their smaller size by occupying the interstices of the frozen glassy matrix, to be revealed as a sub-T_g process at ultraflow frequencies in dielectric measurements. It is suggested that stable complexes of 2:1 and 1:1 exist near T_g in DMSO and EG aqueous solutions, respectively. At concentrations corresponding to these complexes, the dielectric spectrum shows a marked "homogeneity".

Acknowledgment. The author thanks Prof. Deepak Kumar for the helpful discussions and also the Department of Science and Technology (DST), India, for the financial help.

References and Notes

(1) Mittal, K. L., Ed. *Micellization, Solubization and Microemulsions*; Plenum Press: New York, 1977; Vol. 1.
(2) Myers, D. *Surfactant Science and Technology*; VCM Publishers: New York, 1988.
(3) Koga, Y.; Siu, W. Y. W.; Wong, T. Y. H. *J. Phys. Chem.* **1990**, *94*, 3879.
(4) D,Arrigo, D.; Teixeira, J.; Giordano, R.; Mallamace, F. *J. Chem. Phys.* **1991**, *95*, 2732.
(5) Roux, G.; Perron, G.; Desnoyers, J. E. *J. Phys. Chem.* **1978**, *82*, 966.
(6) Leake, C. D., Ed. *Biological Actions of Dimethyl Sulfoxide: Annals of the New York Academy of Sciences*; New York Academy of Sciences: New York, 1967; Vol. 141.
(7) Ashwood, M. J.; Farvant, J. *Low Temperature Preservation in Medicine and Biology*; University Park Press: Baltinole, 1980.
(8) Fuchs, R.; McCrary, G. B.; Bloomfield, J. J. *J. Am. Chem. Soc.* **1961**, *83*, 4281.
(9) Drinkard, W.; Kivelson, D. *J. Am. Chem. Soc.* **1958**, *62*, 1494.
(10) Lindberg, J. J.; Majani, C. *Acta Chem. Scand.* **1963**, *17*, 1477.
(11) Safford, G. J.; Schaffer, P. C.; Leung, D. S.; Doebbler, G. F.; Brady, G. W.; Lyden, E. F. X. *J. Chem. Phys.* **1969**, *50*, 2140.
(12) Cowie, J. M. G.; Toporowski, P. M. *Can. J. Chem.* **1961**, *39*, 2240.
(13) Fort, R. J.; Moore, W. R. *Trans. Faraday Soc.* **1966**, *62*, 1112.
(14) Schickman, S. A.; Amey, R. L. *J. Phys. Chem.* **1971**, *75*, 98.
(15) Kaatze, U.; Pottel, R.; Schafer, M. *J. Phys. Chem.* **1989**, *93*, 5623.
(16) Glasel, J. A. *J. Am. Chem. Soc.* **1970**, *92*, 372.
(17) Higashigaki, Y.; Christiansen, D. H.; Wang, C. H. *J. Phys. Chem.* **1981**, *85*, 2531.
(18) Baker, E. S.; Jonas, J. *J. Phys. Chem.* **1985**, *89*, 1790.
(19) Madigosky, W. M.; Warfield, R. W. *J. Chem. Phys.* **1983**, *78*, 1912.
(20) Petrelia, G.; Petrelia, M.; Castagncio, M.; Dell'Att, A.; Destiglio, A. *J. Solution Chem.* **1981**, *10*, 129.
(21) deVisser, C.; Henvesland, M. J. M.; Dunn, L. A.; Somsen, G. J. *J. Chem. Soc., Faraday Trans.* **1978**, *74*, 1159.
(22) Puranik, S. M.; Kumbharkhane, A. C.; Mehrotra, S. S. *J. Chem. Soc., Faraday Trans.* **1992**, *88*, 433.
(23) Brink, G.; Falk, M. *J. Mol. Struct.* **1970**, *5*, 27.
(24) Allerhand, A.; Schleyer, P. V. R. *J. Am. Chem. Soc.* **1963**, *85*, 371.
(25) Murthy, S. S. N. Submitted.
(26) Rasmussen, D. H.; MacKenzie, A. P. *Nature* **1968**, *220*, 1315.
(27) Timmermans, J. *The Physico-Chemical Constants of Binary Systems in Concentrated Solutions*; Int. Sci. Publ.: New York, 1960; Vol. 4.
(28) Murthy, S. S. N. *J. Phys. Chem.* **1996**, *100*, 8508.
(29) Murthy, S. S. N.; Paikary, A.; Arya, N. *J. Chem. Phys.* **1995**, *102*, 8213.
(30) Havriliak, S.; Negami, S. J. *Poly. Sci. C* **1966**, *14*, 99.
(31) Hasted, J. B. *Aqueous Dielectrics*; Chapman and Hall: London, 1973.
(32) Huck, J. R.; Noyel, G. A.; Jorat, L. J. *IEEE Trans. Electr. Insul.* **1988**, *23*, 627.
(33) (a) Hill, N. E.; Vaughan, W. E.; Price, A. H.; Davies, M. *Dielectric Properties and Molecular Behavior*; Van Nostrand Reinhold: London, 1969. (b) The exact identity can be derived from eq 1 as $f_m = f_0(k/(\cos(\alpha\pi/2) - \sin(\alpha\pi/2)k))^{1/(1-\alpha)}$, where $k = \tan((1 - \alpha)\pi/2(1 + \beta))$, which for small α can be approximated as $f_m = f_0 \tan(\pi/2(1 + \beta))$.
(34) Lesikar, A. *J. Chem. Phys.* **1977**, *66*, 4263.
(35) Buckley, F.; Maryott, A. A. "*Tables of Dielectric Dispersion Data for Pure Liquids and Dilute Solutions*"; National Bureau of Standards Circular 589; 1958.
(36) Rasmussen, D. H.; MacKenzie, A. P. *J. Phys. Chem.* **1971**, *75*, 967.
(37) Mashimo, S.; Umehara, T.; Redlin, H. *Chem. Phys.* **1991**, *95*, 6257.
(38) Reid, R. C.; Prausitz, J. M.; Poling, B. E. "*The Properties of Gases and Liquids*", 4th ed.; McGraw Hill: Singapore, 1988.
(39) Murthy, S. S. N.; Sobhanadri, J.; Gangasharan. *J. Chem. Phys.* **1994**, *100*, 4601.
(40) Gangasharan; Murthy, S. S. N. *J. Phys. Chem.* **1995**, *99*, 12349.
(41) Murthy, S. S. N. *Phase Transitions* **1994**, *50*, 63.
(42) Von Hippel, A. IEEE Trans. Electron Insul. **1988**, *32*, 801.
(43) Nayak, S. K.; Murthy, S. S. N. *J. Chem. Phys.* **1993**, *99*, 1607.
(44) Gangasharan; Murthy, S. S. N. *J. Chem. Phys.* **1993**, *99*, 9865.
(45) Hedvig, P. *Dielectric Spectroscopy of Polymers*; Adam Hilger Ltd.: Bristol, 1977.
(46) Jorat, L. J.; Noyel, G. A.; Huck, J. R. IEEE Trans. Electron Insul. **1991**, *26*, 763.
(47) Mashimo, S.; Miura, N. *J. Chem. Phys.* **1993**, *99*, 9874.
(48) Lesikar, A. V. *Phys. Chem. Glasses* **1975**, *16*, 83.
(49) Lai, J. T. W.; Lau, F. W.; Robb, D.; Werth, P.; Nielsen, G.; Trandum, C.; Hvidt, A.; Koga, Y. *J. Solution Chem.* **1995**, *24*, 89.
(50) Huot, J. Y.; Battisel, E.; Lumry, R.; Villeneuves, G.; Lavallee, J. F.; Anusiem, A.; Jolicoeur, C. *J. Solution Chem.* **1988**, *17*, 601.
(51) Tanaka, S. H.; Yoshihara, H. I.; Wen-Chi Ho, A.; Lau, F. W.; Westh, P.; Koga, Y. *Can. J. Chem.* **1996**, *74*, 713.